

## Propagation Effects on Reflectivity for Circularly Polarized S-Band Radars

ENRICO TORLASCHI AND BERNARD PETTIGREW

*Département de Physique, Université du Québec à Montréal, Québec, Canada*

(Manuscript received 3 April 1989, in final form 11 August 1989)

### ABSTRACT

The effect of the propagation medium on the measurements of the radar reflectivity factor for circularly polarized S-band radar is assessed using model storms. The results show that for convective cells, the propagation effects can lead to underestimation of the reflectivity factor by an amount that is of the same order of magnitude as the attenuation at C-band.

### 1. Introduction

The polarization state of transmitted microwaves has recently become a subject of interest due to the promise of an increase in the number of applications of polarization diversity. The NEXRAD (Next Generation Weather Radar) prototype radar, for example, includes transmitted circular polarization although reception in one channel only is available at first. The use of circular polarization has the disadvantage that propagation through heavy rain can seriously depolarize a 3 GHz wave (Humphries 1974), and the interpretation of the polarization parameter observations in such regions must be made with some estimate of the strength of these propagation effects. However, little attention has been paid to the effect of the interactions of circular polarized waves and rain on reflectivity.

Sections 2 and 3 present a review of the relations for determining the effective reflectivity factors using circular polarization base vectors. Model storms are used in section 4 to assess the influence of the propa-

gation medium on the measurements of the radar reflectivity factor for S-band circular polarized radars if only cross-polar signal power is available.

### 2. Summary of equations

From the work of McCormick and Hendry (1975) it follows that at circular polarization the received electric field,  $[E_+, E_-]^t$ , from a single particle is given by

$$\begin{bmatrix} E_+ \\ E_- \end{bmatrix}^t = P^T S P \begin{bmatrix} M_+ \\ M_- \end{bmatrix}^t, \quad (1)$$

where the subscripts + and - indicate right-hand circular (RHC) polarization and left-hand circular (LHC) polarization, respectively;  $[M_+, M_-]^t$  denotes the transmitted wave amplitudes;  $S$  and  $P$  designate the backscatter matrix and the propagation matrix, respectively; and  $P^T$  is the transpose of  $P$ .

If the particle has an axis of symmetry, the backscatter matrix  $S$  can be shown to be

$$S = \begin{bmatrix} (S_{xx} - S_{yy} - j2S_{xy})e^{j2\alpha} & S_{xx} + S_{yy} \\ S_{xx} + S_{yy} & (S_{xx} - S_{yy} + j2S_{xy})e^{-j2\alpha} \end{bmatrix}, \quad (2)$$

where  $S_{xx}$ ,  $S_{yy}$  and  $S_{xy}$  are the elements of the backscatter matrix assuming linear polarization basis, and  $\alpha$  is the canting angle of the particle axis of symmetry with respect to the vertical.

Assuming that the two polarizations that propagate through the medium without depolarization are linear

and orthogonal, the propagation matrix  $P$  is given by

$$P = \underbrace{\frac{e^{-\gamma(r)}}{r}}_A \underbrace{\frac{1}{\sqrt{1 - (pe^{jx})^2}} \begin{bmatrix} 1 & pe^{j(x-2r)} \\ pe^{j(x+2r)} & 1 \end{bmatrix}}_B \quad (3)$$

with

$$\gamma(r) = j \frac{\gamma_1(r) + \gamma_2(r)}{2} \quad (4)$$

*Corresponding author address:* Dr. Enrico Torlaschi, Département de Physique, Université du Québec à Montréal, Case postale 8888, succursale A, Montréal, Québec, H3C 3P8, Canada.

and

$$pe^{jx} = \tanh \left[ j \frac{\gamma_1(r) - \gamma_2(r)}{2} \right], \quad (5)$$

where  $r$  is the range,  $\gamma_1(r)$  and  $\gamma_2(r)$  are the propagation functions (section 3) along a set of axes corresponding to the two characteristic polarizations, and  $\tau$  is the angle of these axes with respect to the vertical. The angle  $\tau$  is determined by the mean canting angle of the particles filling the propagation path.

In (3), term A is the attenuation of the signal and term B corresponds to the propagation effects due to the differential phase propagation and the differential attenuation between the two characteristic polarizations.

When circularly polarized radiation is transmitted toward an ensemble of particles uniformly filling a radar resolution volume, the cross-polar signal power,  $W_2$ , of the received wave is given by

$$W_2 = |C|^2 \langle |E_{\pm}|^2 \rangle, \quad (6)$$

where  $C$  is a radar-related constant, the plus sign refers to transmission of LHC polarization and the minus sign to transmission of RHC polarization, and the angle brackets represent the ensemble averages over shapes, orientations, and sizes.

By a combination of (1) thru (6), it is found that

$$W_2 = |C|^2 \frac{e^{-A}}{4\pi r^2} \frac{1}{|1 - p^2 e^{j2x}|^2} \langle \sigma_c |1 + p^2 e^{j2x} + \eta^- p e^{j(x+2\tau)} + \eta^+ p e^{j(x-2\tau)}|^2 \rangle, \quad (7)$$

where  $A = 4 \operatorname{Re}[\gamma(r)]$  specifies the mean attenuation of the radar signal,  $\sigma_c = \pi |S_{xx} + S_{yy}|^2$  is the backscatter cross section at circular polarization, and  $\eta^{\pm}$  is given by

$$\eta^{\pm} = \frac{S_{xx} - S_{yy} \mp j2S_{xy}}{S_{xx} + S_{yy}} e^{\pm j2\alpha}. \quad (8)$$

The effective reflectivity factor from radar measurements that is commonly used to characterize the scattering ensemble is given by

$$\tilde{Z}_e = \frac{\lambda^4}{\pi^5 |K|^2} \frac{4\pi r^2}{|C|^2} W_2, \quad (9)$$

while the equivalent reflectivity factor of an assembly of hydrometeors is defined for circular polarization as

$$Z_e = \frac{\lambda^4}{\pi^5 |K|^2} \langle \sigma_c \rangle, \quad (10)$$

where  $\lambda$  and  $K$  have the usual meaning.

From (7), (9), and (10) it appears that only when the signal depolarization and the attenuation can be neglected ( $p \approx 0$  and  $A \approx 0$ ), the effective reflectivity factor measured by the radar,  $\tilde{Z}_e$ , is equal to  $Z_e$ .

### 3. The propagation functions

The difference between the measured reflectivity (9) and the intrinsic reflectivity (10) is cumulative with range when the propagation medium is anisotropic. In order to assess this effect we must express  $E_{\pm}$  in (6) as a function of the distance that the wave travels within the medium.

A region of precipitation composed of nonspherical particles with a preferred orientation constitutes an anisotropic propagation medium. Furthermore, the spatial variability of the precipitation rate implies variations of the anisotropy with range. Therefore, precipitation constitutes a nonuniform anisotropic medium and special consideration has to be given to the determination of the two propagation functions  $\gamma_1(r)$  and  $\gamma_2(r)$ .

If the mean canting angle,  $\tau$  of the particles filling the propagation path as well as the permeability,  $\mu$ , are independent of range, and the plane of polarization is orthogonal to the gradient of the permittivity,  $\epsilon$ , then Maxwell's equations lead to the following wave equation:

$$\nabla^2 \vec{E} + k^2(r) \vec{E} = 0, \quad (11)$$

where  $k(r) = \omega[\mu\epsilon(r)]^{1/2}$  and  $\omega$  is the frequency of oscillation.

At a distance from the source where  $r \gg \lambda$ , any portion of a spherical wave surface is essentially a plane wave traveling in the  $r$  direction. Thus, (11) becomes

$$\frac{1}{r^2} \frac{\partial}{\partial r} \left( r^2 \frac{\partial E_i}{\partial r} \right) + k_i^2(r) E_i = 0; \quad i = 1, 2, \quad (12)$$

where  $E_i$  ( $i = 1, 2$ ) represent the two linear and orthogonal polarizations that propagate through the medium without depolarization, and  $k_i$  ( $i = 1, 2$ ) are the two corresponding propagation constants of a thin plane-parallel slab containing a large population of particles distributed uniformly in space.

The exact solution of (12) may be some unknown function of great complexity. Nevertheless, a suitable assumption for precipitation is that  $k_i^2(r)/\lambda^2$  ( $i = 1, 2$ ) are slowly varying with respect to the wavelength. In this case, the asymptotic solution of (12) is readily obtained using the WKB method (Mathews and Walker 1970):

$$E_i = \frac{E_{0i}}{r} \exp \left\{ -j \left[ \int_0^r k_i(r) dr + \frac{j}{2} \ln \frac{k_i(0)}{k_i(r)} \right] \right\} \\ = \frac{E_{0i}}{r} e^{-j r_i(r)}; \quad i = 1, 2, \quad (13)$$

where  $E_{0i}$  ( $i = 1, 2$ ) represent the rectangular components of the transmitted field and the propagation functions are

$$\gamma_i = \int_0^r k_i(r) dr + \frac{j}{2} \ln \frac{k_i(0)}{k_i(r)}; \quad i = 1, 2. \quad (14)$$

Using the theory in van de Hulst (1957), it can be shown that the propagation constants are related to the forward scattering amplitudes,  $S_{ii}(0)$ :

$$k_i = k_0 + \frac{2\pi}{k_0} \langle S_{ii}(0) \rangle; \quad i = 1, 2, \quad (15)$$

where  $k_0 = 2\pi/\lambda$  is the free-space propagation constant.

**4. Calculations of the effective reflectivity factor**

We will assess next the influence of the propagation medium on the measurements of the radar reflectivity at S-band, using two models of precipitation:

- (i) widespread uniform rain, and
- (ii) a model convective cell with linear increase and decrease with range of logarithm of the rain rate (hereafter designated by triangular rain; Fig. 2a).

As in Torlaschi et al. (1984), the scattering amplitudes are calculated from oblate spheroidal models of raindrops using Gans scattering theory (van de Hulst 1957) for a Marshall and Palmer (1948) drop size distribution with relationship between size and shape given by Pruppacher and Pitter (1971). Moreover, the distribution of canting angle about  $\alpha = 0^\circ$  is supposed to be Gaussian with standard deviation,  $\sigma_\alpha$ , as a function of diameter,  $D$ , given by

$$\sigma_\alpha = \begin{cases} 90e^{-0.95D^2}, & D \leq 2 \text{ mm} \\ 2, & D > 2 \text{ mm}. \end{cases} \quad (16)$$

The inclination angle of the axes of anisotropy,  $\tau$ , is assumed to be zero.

The form of  $\sigma_\alpha$  in (16) is rather arbitrary, but (i) it incorporates the idea that small raindrops are more randomly oriented, and (ii) as shown in Torlaschi (1983), its use in the calculations of the polarization parameters improves the agreement between them and the rain depolarization measurements reported by McCormick and Hendry (1976).

Thus, if the rainfall rate is specified as a function of range,  $Z_e$  and  $\tilde{Z}_e$  can be calculated at every range by the following sequence of the previously derived equations:

- 1) The rainfall rate is used to obtain the drop size distribution.
- 2) For each drop the scattering amplitudes are calculated.
- 3) The forward scattering amplitudes are introduced in (15) to calculate  $k_i$  ( $i = 1, 2$ ).
- 4) The variation of  $k_i$  with distance is used in (14) to calculate the propagation functions  $\gamma_i$  ( $i = 1, 2$ ).
- 5)  $\gamma(r)$  and  $pe^{\beta x}$  are then calculated from (4) and (5).
- 6)  $\eta^\pm$  and  $\sigma_c$  are calculated using the backward scattering amplitudes.

- 7)  $W_2$  is calculated from (7).
- 8)  $\tilde{Z}_e$  is calculated introducing  $W_2$  in (9).
- 9)  $Z_e$  is calculated introducing  $\sigma_c$  in (10).

Figure 1 shows the difference between  $Z_e$  and  $\tilde{Z}_e$  as a function of range for the uniform rain model with a rainfall rate,  $R$ , of  $4 \text{ mm h}^{-1}$  ( $Z_e \approx 32 \text{ dBZ}$ ). For comparison with the propagation effect due to the differential phase shift and the differential attenuation, this figure gives also the attenuation at 10 cm. As can be seen, the influence of the propagation effects (difference between the solid and the dotted curves) is slight: about 0.2 dB at a range of 200 km.

Figure 2b shows  $Z_e$  and  $\tilde{Z}_e$  as a function of range for a triangular rain model of 50 km extent, with  $200 \text{ mm h}^{-1}$  rain rate in the middle and  $1 \text{ mm h}^{-1}$  at both ends (Fig. 2a). In Fig. 3 the difference between  $Z_e$  and  $\tilde{Z}_e$  as a function of range is presented. For comparison the attenuations at S-band and C-band are shown as well. At C-band the radar specific attenuation,  $Y$ , is calculated as (Wexler and Atlas 1963):

$$Y (\text{dB km}^{-1}) = 0.003R (\text{mm h}^{-1}). \quad (17)$$

It appears from Fig. 3 that up to 25 km (the range of the maximum rain rate,  $R_{\text{max}}$ ) the power loss due to the propagation effects is moderate but still permits a fair estimation of  $R_{\text{max}}$ . On the other hand, in the far side of the precipitation the propagation effects on the S-band circularly polarized waves become as severe as the attenuation of C-band waves. Therefore, the precipitation in the shadow of a convective cell (e.g.,

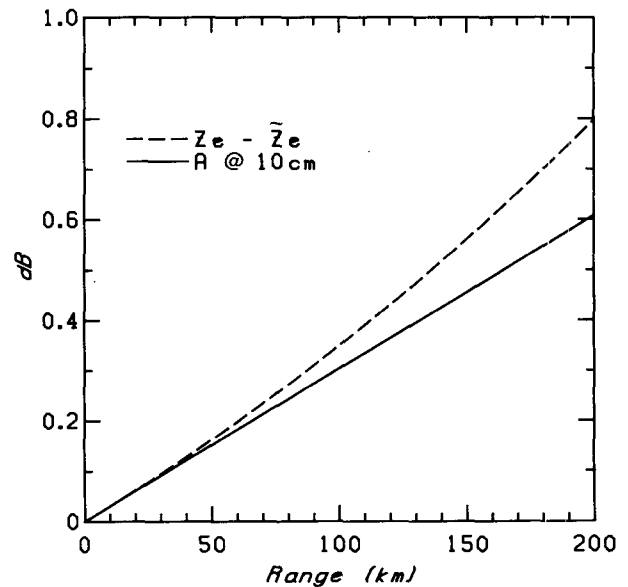


FIG. 1. Dashed line:  $Z_e - \tilde{Z}_e$  as a function of range for a uniform rain model with a rain rate of  $4 \text{ mm h}^{-1}$  ( $Z_e \approx 32 \text{ dBZ}$ ). The solid line corresponds to radar attenuation at 10.4 cm.

other convective cells) cannot be quantitatively evaluated until the leading cell moves aside.

**5. Conclusions**

Two model storms are used to assess the influence of the propagation medium on the measurements of the radar reflectivity factor for S-band circular polarized radars if only cross-polar signal power is available as in the NEXRAD prototype radar.

From our calculations it is seen that for widespread moderate rain with uniform rainfall rate of  $4 \text{ mm h}^{-1}$ , the influence of the signal depolarization on reflectivity is about 0.2 dB at a range of 200 km; i.e., three times less severe than the signal losses due to attenuation only. For the model convective cell shown in Fig. 2a, the signal depolarization at the far side of the cell engenders signal losses of about 4.5 dB. This is more than five times worse than signal loss by attenuation only at S-band. In this case, the total signal losses are comparable to attenuation at C-band. Because the propagation effects are cumulative with range, the equivalent reflectivity factor for circular polarization cannot be quantitatively evaluated especially if the radar happens

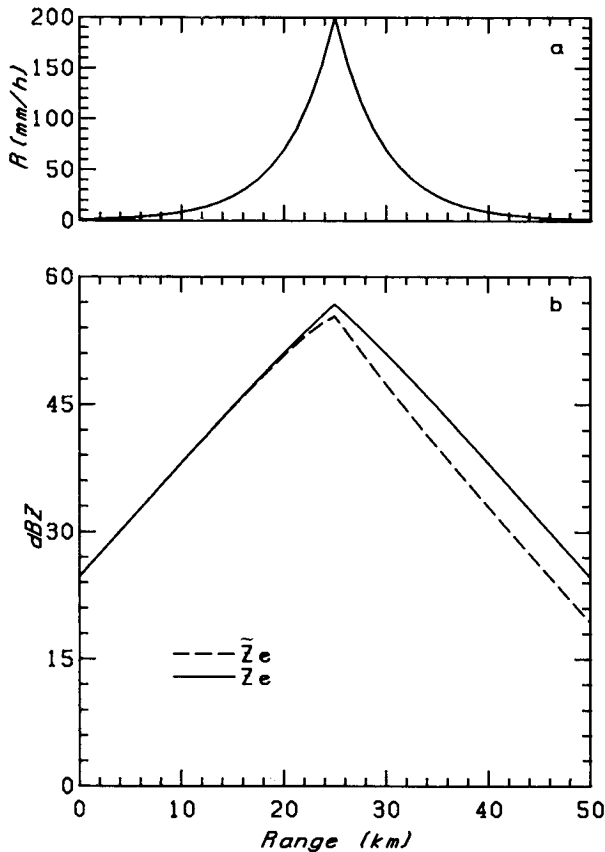


FIG. 2. (a) Model convective cell: Rain rate as function of range. (b) Solid line  $Z_e$ , and dashed line  $\tilde{Z}_e$  for the triangular rain model in (a).

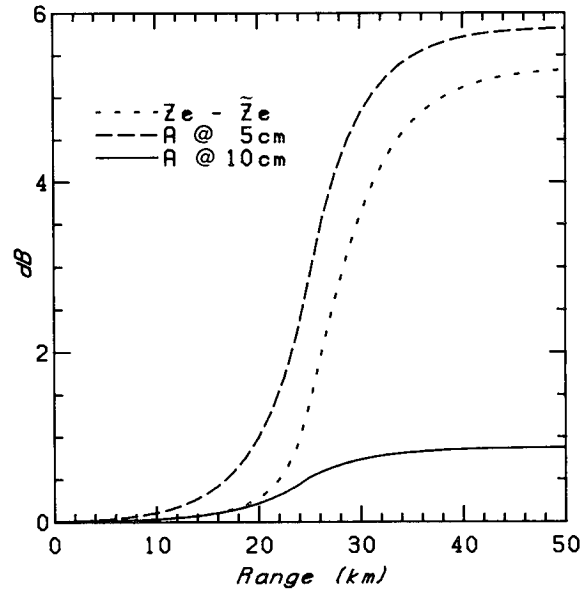


FIG. 3. Dotted line:  $Z_e - \tilde{Z}_e$  as a function of range for the triangular rain model as in Fig. 2a. The solid and dashed lines correspond to radar attenuation at 10.4 and 5.7 cm, respectively.

to observe severe storms through a line. Therefore, there is advantage in choosing linear rather than circular polarization when only the cross-polar signal power is available.

*Acknowledgments.* This work was partially supported by the National Sciences and Engineering Research Council of Canada, and by the Atmospheric Environment Service Department of the Environment Canada.

REFERENCES

Humphries, R. G., 1974: Observations and calculations of depolarization effects at 3 GHz due to precipitation. *J. Rech. Atmos.*, **8**, 155-161.

Marshall, J. S., and W. McK. Palmer, 1948: The distribution of raindrops with size. *J. Meteor.*, **5**, 165-166.

Mathews, J., and R. L. Walker, 1970: *Mathematical Methods of Physics*. The Benjamin/Cummings Publishing Company, 501 pp.

McCormick, G. C., and A. Hendry, 1975: Principles for radar determination of the polarization properties of precipitation. *Radio Sci.*, **10**, 421-434.

—, and A. Hendry, 1976: Polarization-related parameters for rain: Measurements obtained by radar. *Radio Sci.*, **11**, 731-740.

Pruppacher, M. R., and R. L. Pitter, 1971: A semi-empirical determination of the shape of cloud and rain drops. *J. Atmos. Sci.*, **28**, 86-94.

Torlaschi, E., 1983: Potential use of circular depolarization measurements for inference of raindrop and hailstone size distributions. *Proc. 21st Conf. Radar Meteor.*, Edmonton, Amer. Meteor. Soc., 454-458.

—, R. G. Humphries and B. L. Barge, 1984: Circular polarization for precipitation measurement. *Radio Sci.*, **19**, 193-200.

van de Hulst, H. C., 1957: *Light Scattering by Small Particles*. John Wiley and Sons, 470 pp.

Wexler, R., and D. Atlas, 1963: Radar reflectivity and attenuation of rain. *J. Appl. Meteor.*, **2**, 276-280.